Enhanced DC-Link Voltage Regulation of Autonomous Squirrel Cage Generators with Iron Losses Consideration in Wind-Powered Conversion Plants using Direct Power Control, Type-2 Fuzzy Logic Control, and Flower Pollination Algorithm Optimization

Ouafia Fadi*‡, Ahmed Abbou*, Hassane Mahmoudi*, Soufiane Gaizen*

*Electrical Engineering Department, Mohammadia School of Engineers, Mohammed V University, Rabat, 10090, Morocco

(fadiouafia@gmail.com, abbou@emi.ac.m, mahmoudi@emi.ac.ma, soufiane.gaizen@gmail.com)

‡Corresponding Author; Ouafia Fadi, 10090 Tel: +212 6 60 87 00 22, fadiouafia@gmail.com

Received: 01.08.2023 Accepted:12.09.2023

Abstract- In the realm of sustainable energy generation, Autonomous Squirrel Cage Generators (ASCGs) are indispensable due to their cost-effectiveness. However, ensuring precise DC-link voltage (V-DC) regulation in ASCGs, especially under varying conditions, remains a critical challenge. This study introduces a novel control strategy employing the Direct-Power-Controller (DPC) in conjunction with Type-2 Fuzzy-Logic Controller (T2FLC), augmented by the Flower-Pollination-Algorithm (FPA). Quantitative analysis reveals substantial enhancements in critical performance metrics under constant reference conditions, including a 1.1% reduction in rise time, a 5.03% decrease in settling time, a 0.06% increase in power factor (PF), and a 5.14% reduction in total harmonic distortion (THD). Moreover, under variable reference conditions, the proposed controller demonstrates exceptional responsiveness and establishes a linear relationship between V-DC and active power, with smooth transitions. In scenarios with variable wind speeds, the controller outperforms alternatives, exhibiting significant improvements in settling times. These findings underscore the efficacy of the T2FLC+DPC controller, optimized through FPA, for precise DC voltage regulation in ASCGs, presenting valuable implications for renewable energy systems and power electronics control. This study contributes quantitative insights that highlight the controller's potential to enhance ASCG performance, thus promoting the wider adoption of sustainable energy solutions.

Keywords ASCGs, DPC, FPA, Iron losses, T1FLC, T2FLC, Wind power.

1. Introduction

Embracing renewable energy systems presents a practical and sustainable alternative to our current reliance on fossil fuels, The depletion of finite fossil fuel reserves, coupled with their detrimental impact on climate change, necessitates a shift towards renewable sources [1]. The incorporation of clean energy systems is therefore critical in addressing the growing demand for energy while reducing carbon emissions [2]. In recent times, there has been a surge in the adoption of renewable energy systems across the globe, driven by factors such as technological advancements, government incentives, and public understanding of ecological concerns [3]. Wind turbines and solar panels have gained popularity due to their ability to generate clean energy from renewable sources [4]. As a result, numerous nations and institutions have established ambitious goals aimed at enhancing the proportion of renewable energy within their energy portfolio, highlighting

the growing importance of renewable energy systems in the global energy landscape [5]. In the realm of renewable energy, wind power has emerged as a highly consequential player in recent years, capturing substantial attention due to its inherent potential to generate electricity in an environmentally friendly and sustainable manner [6]. Wind energy systems commonly encompass aerogenerators, specialized devices that harness the kinetic power of wind and convert it into usable electrical energy [7]. However, selecting the appropriate type of generator for a wind energy system is critical for its efficient and reliable operation. Autonomous Squirrel Cage Generators (ASCGs) have emerged as a promising solution for small-scale wind energy applications, offering several advantages over other types of generators [8]. ASCGs are preferred for small-scale wind energy applications due to their low cost, simple construction, ability to operate in variable speed conditions, and high efficiency in power conversion [9]. However, the unstable DC-link voltage is a critical issue for the reliable and stable operation of ASCGs in wind energy systems [10].

This is particularly challenging because ASCGs operate at variable speeds and under varying load conditions, which can cause voltage fluctuations. Improving the voltage regulation of ASCGs is essential to prevent these instabilities and ensure efficient energy conversion [11]. Various control methods have been proposed in the literature [12] to ensure the stable and reliable operation of the ASCG. These control techniques aim to improve the DC-link voltage regulation of this machine in wind energy systems. These methods include fuzzy logic control [13], neural network-based control [14], adaptive control [15], and model predictive control [16], among others. Dewangan. S. [17] proposed a model for monitoring the autonomous excited squirrel cage Generator using indirect vector control. The system uses a two-level back-to-back converter to separately regulate torque, active power, reactive power, and DC voltage for distinct wind speeds. The application of a fuzzy logic controller as a substitute for a PI controller improves system response during changes in wind speed. Simulation results demonstrate the superiority of the FL controller over the PI controller for variable speed operations. Dagang. C [18] unveiled a revolutionary direct-fuzzy-control model for wind power generation systems. This pioneering model seamlessly incorporates the direct-fuzzy-torque and power control laws, thereby exhibiting a profound impact on the quality of energy produced. By employing the direct fuzzy torque control law, the control signal for the generator-side converter is derived, ensuring precise and adaptive control. Simultaneously, the utilization of the direct fuzzy power control law on the grid side endeavors to achieve an unparalleled level of power efficiency. Distinct from conventional direct control methods, this proposed approach transcends expectations by delivering exceptional trajectory tracking capabilities and unrivaled resilience to fluctuations in the generator's internal parameters.

Bendjeddou. Y [19] introduces a novel virtual flux-based control (VFC) incorporating nonlinear super-twisting sliding mode control (STSMC) to optimize autonomous squirrel cage generators (ASCG) in wind energy plants. This strategy, coupled with space-vector modulation (SVM) integrated into pulse width modulation (PWM) rectifiers, improves system dynamics while reducing current distortions. Dyanamina. G [20] introduces a control model for standalone Pico-electric power plant generators. This model deploys a fuzzy logic controller (FLC) with a static compensator (STATCOM) to manage reactive power fluctuations in autonomous squirrel cage generators (ASCGs), ensuring voltage stability. MATLAB/Simulink simulations validate this innovative scheme. Esquivel-Sancho.L [21] has devised a sophisticated modeling approach within the port-Hamiltonian framework, tailored specifically for autonomous squirrel cage Generators. This comprehensive framework not only captures the intricate dynamics of these generators but also paves the way for a pioneering control law. This control strategy is meticulously designed to regulate voltage with unparalleled precision, and its foundation lies in an intricate trajectory-tracking strategy. This innovative approach promises to enhance the performance and stability of autonomous squirrel cage Generators, making significant strides in the field of renewable energy systems. Sombir.S [22] presents an advanced voltage-frequency (VF) controller tailored for autonomous squirrel cage Generators (ASCGs) in conjunction with a photovoltaic (PV) system at the DC link, accommodating diverse linear and nonlinear loads. This multifaceted VF controller features a sophisticated 4-leg IGBT-based current-controlled voltage source converter (CC-VSC), complemented by a dump load and an integrated PV system. Its primary mission is to ensure uninterrupted operational stability, maintaining a constant voltage and frequency regardless of dynamic load fluctuations. Sombir.S's innovative approach not only promises to optimize energy generation and consumption but also underscores the pivotal role of precision control strategies in the dynamic landscape of renewable energy systems. Despite significant advancements in the field of ASCG control, achieving stable and efficient DC-link voltage regulation remains a persistent challenge, particularly in the face of variable load and speed conditions [23, 24]. This challenge stems from the intrinsic nonlinear and time-varying properties of ASCGs, as well as the uncertainties associated with wind speed and other operational parameters [25]. As a result, the development of effective control strategies to address these issues and ensure reliable power generation from ASCGs has recently gained significant traction as a dynamic field of research. Traditional PI controllers and Type-1 Fuzzy-Logic-Controllers (T1FLCs) have been extensively employed for ASCG voltage regulation, but they may not be able to handle the complexity and variability of ASCGs. Therefore, there is a need for advanced control techniques that can effectively manage the voltage generated by the DC-link.

In the pursuit of reliable and sustainable energy solutions, Autonomous Squirrel Cage Generators (ASCGs) have gained prominence for their cost-effectiveness. Nevertheless, the challenge of maintaining stable operation, especially under dynamic load and speed conditions, remains a pressing concern. This paper presents an innovative and robust control methodology, uniting Direct-Power-Control (DPC), Type-2 Fuzzy-Logic-Controller (T2FLC), and the Flower-Pollination-Algorithm (FPA). Our primary objective is to advance the management of DC-link voltage in three-phase

ASCGs, effectively addressing the complex, non-linear dynamics of these systems and accounting for uncertainties in wind speed and operating loads. DPC provides precise and swift power control, while T2FLC excels in handling uncertainties and adapting to changing conditions. Leveraging the FPA to optimize T2FLC's membership functions further enhances control performance. Through rigorous simulation, we substantiate our proposed scheme's superiority over conventional PI and T1FLC controllers. This research not only optimizes ASCG performance but also signifies a promising stride toward efficient and adaptive energy generation. We believe these findings are instrumental in advancing the field of renewable energy systems and power electronics control, addressing key industry challenges, and promoting a more sustainable energy landscape.

2. Autonomous Squirrel Cage Generator Modelling

2.1. D-Q Axes ASCG Mathematical Model

The ASCG mathematical model deviates from that of a typical induction motor due to the inclusion of a capacitor bank. Within the d-q reference frame, the equations governing the stator and rotor flux, voltage, and air gap flux are formulated and expressed as primary variables, distinguishing the ASCG from its traditional counterpart. The classic d-q model of the asynchronous machine can be presented as follows [26, 27]:

$$u_{sd} = R_s i_{sd} + \frac{d\psi_{sd}}{dt} - \omega_a \psi_{sq} \quad (1)$$

$$u_{sq} = R_s i_{sq} + \frac{d\psi_{sq}}{dt} - \omega_a \psi_{sd} \quad (2)$$

$$u_{rd} = R_r i_{rd} + \frac{d\psi_{rd}}{dt} - (\omega_a - \omega)\psi_{rq} \quad (3)$$

$$u_{rq} = R_r i_{rq} + \frac{d\psi_{rq}}{dt} - (\omega_a - \omega)\psi_{r4} \quad (4)$$

$$\psi_{sd} = L_s i_{sd} + L_m i_{rd} \quad (5)$$

$$\psi_{sq} = L_s i_{sq} + L_m i_{rq} \quad (6)$$

$$\psi_{rd} = L_r i_{rd} + L_m i_{sd} + \psi_{rd0} \quad (7)$$

$$\psi_{rq} = L_r i_{rq} + L_m i_{sq} + \psi_{rq0} \quad (8)$$

$$i_{md} = i_{sd} + i_{rd} \quad (9)$$

$$i_{mq} = i_{sq} + i_{rq} \quad (10)$$

$$T_m = \frac{3}{2} p \frac{L_m}{L_r} \left(\psi_{rd} i_{sq} - \psi_{rq} i_{sd}\right) \quad (11)$$

with:

$u_{sd}, u_{sq}, u_{rd}, u_{rq}$: dq components of stator and rotor voltage vectors,
$i_{sd}, i_{sq}, i_{rd}, i_{rq}$: dq components of stator and rotor current vectors,
$\psi_{sd}, \psi_{sq}, \psi_{rd}, \psi_{rq}$: dq components of stator and rotor magnetic flux vectors,
ψ_{rd0}, ψ_{rq0} : are the rotor's remanent magnetic fluxes in the d and q axes, respectively.
i_{md}, i_{mq}: dq components of the magnetizing current vector,
R_s, R_r: stator and rotor resistance
L_m, L_s, L_r: Magnetizing stator and rotor inductances, respectively.
p: the pole pairs number.
T_m: electromagnetic torque.
It is also necessary to introduce equations of the load and capacitor voltages and the current consumed.

$$u_{cd} = \frac{1}{C}\int_0^t i_{cd} dt + u_{sd0} \quad (12)$$

$$u_{cq} = \frac{1}{C}\int_0^t i_{cq} dt + u_{sq0} \quad (13)$$

$$u_{Ld} = R_L i_{Ld} \quad (14)$$

$$u_{Lq} = R_L i_{Lq} \quad (15)$$

$$i_{sd} = i_{Ld} + i_{cd} \quad (16)$$

$$i_{sq} = i_{Lq} + i_{cq} \quad (17)$$

Where the terms u_{sd0} and u_{sq0} represent the initial voltages across the capacitor in the d and q axes, respectively.

2.2. Development of ASCG mathematical model with iron loses.

To increase the dynamic model's accuracy for an asynchronous machine, it becomes imperative to incorporate iron losses into the model. However, this inclusion inevitably results in increased complexity. Thus, it becomes crucial to strike a balance between simplicity and accuracy. In the case of the ASCG, representing iron losses as a constant parameter proves insufficient in attaining the desired level of accuracy. Instead, a resistance term, denoted as Rm, is introduced into the model [28]. This modification is visually depicted in Fig. 1. To determine the equivalent circuit, the Thevenin transformation technique [29] is employed. By adopting this approach, the model successfully accommodates the effect of iron losses with a reasonable level of complexity, thereby ensuring accurate simulation results.

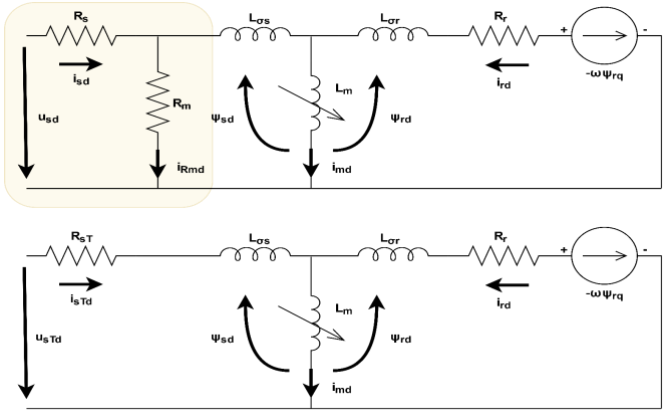

Fig. 1. Equivalent diagram of the autonomous squirrel cage generator in a dq reference frame with consideration of iron losses.

The pre-existing equations will remain applicable to this model, given that the annotations are updated to incorporate the Thevenin transformation [30].

$$R_{sT} = R_s \parallel R_m = \frac{R_s R_m}{R_s + R_m} \tag{18}$$

$$u_{sTd} = u_{sd}\frac{R_m}{R_s + R_m} \tag{19}$$

$$u_{sTq} = u_{sq}\frac{R_m}{R_s + R_m} \tag{20}$$

$$i_{sTd} = i_{sd}\frac{R_s + R_m}{R_m} + \frac{u_{sd}}{R_m} \tag{21}$$

$$i_{sTq} = i_{sq}\frac{R_s + R_m}{R_m} + \frac{u_{sq}}{R_m} \tag{22}$$

The equations governing the operation are as follows.

$$si_{sTd} = \frac{1}{\sigma L_s L_r}(L_m^2 \omega i_{sTq} - L_r R_{sT} i_{sTd} + L_m \omega L_r i_{rq} + L_m R_r i_{rd} - L_r u_{sTd} - L_m K_{rd}) \tag{23}$$

$$si_{sTq} = \frac{1}{\sigma L_s L_r}(-L_m^2 \omega i_{sTd} - L_r R_{sT} i_{sTq} - L_m \omega L_r i_{rd} + L_m R_r i_{rq} - L_r u_{sTq} - L_m K_{rq}) \tag{24}$$

$$si_{rd} = \frac{1}{\sigma L_s L_r}(-L_s L_m \omega i_{sTq} + L_m R_{sT} i_{sTd} - L_s \omega L_r i_{rq} - L_s R_r i_{rd} + L_m u_{sTd} - L_s K_{rd}) \tag{25}$$

$$si_{rq} = \frac{1}{\sigma L_s L_r}(L_s L_m \omega i_{sTd} + L_m R_{sT} i_{sTq} + L_s \omega L_r i_{rd} - L_s R_r i_{rq} + L_m u_{sTq} - L_s K_{rq}) \tag{26}$$

The coefficient of dispersion of BLONDEL, denoted by σ, is computed using the subsequent formula:

$$\sigma = \frac{L_s L_r - L_m^2}{L_s L_s} \tag{27}$$

Figure 2 shows Rm illustrated as function of both iron losses current iRm and frequency F, obtained through interpolation of the measurement points.

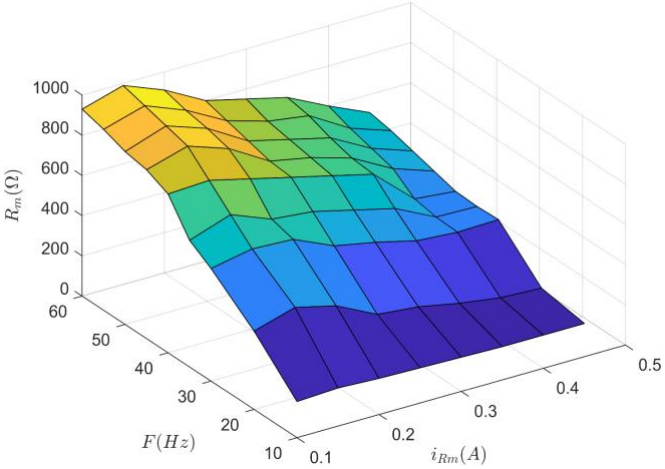

Fig. 2. Evolution of iron losses resistance as function of current and frequency.

3. Enhanced Intelligent DPC Approach for DC Voltage Control

3.1. Type 2 Fuzzy Controller Model

The Traditional Fuzzy Logic Controller (T1FLC) is a control structure utilized to deal with vagueness and ambiguity in nonlinear systems, but its crisp Membership-Functions (MFs) restrict its ability to model uncertainties directly. In contrast, the T2FLC is an extension of T1FLC, which can handle both numeric and linguistic uncertainties. T2FLC makes use of unlimited type-1 MFs throughout a particular band to effectively remove undesirable situations in the controlled setup. To make T2FLC less complex, the auxiliary memberships are set to 1 in interval type-2 fuzzy systems. This paper encompasses an in-depth analysis of the utilization and application of zero-ordered Type-2 Takagi-Sugeno Kang (TSK) fuzzy standards, as discussed in references [31-33], which effectively address the limitations of T1FLC. The T2FLC receives two inputs: the DC-link voltage's error (e) and its change rate (Δe). For this research, the approach taken involves utilizing a type-2 fuzzy membership function of Gaussian form (Figure 3) with a standard deviation that has a level of uncertainty. The mathematical expression for a Gaussian-type membership function is as follows:

$$\mu_{\tilde{B}_i^j} = exp\left[-\frac{1}{2}\left(\frac{x_i - z_i^j}{\sigma_i^j}\right)^2\right] \tag{28}$$

The equations utilize σ and z as symbols for the input vector's midpoint and breadth of the Gaussian membership functions. These parameters are restricted to particular intervals, and solely one of them is regarded as uncertain to avoid an overly extensive parameter space. Fig. 3 illustrates the membership functions forms applied to DC-link voltage's error "e" and the variation in DC-link voltage's error "Δe".

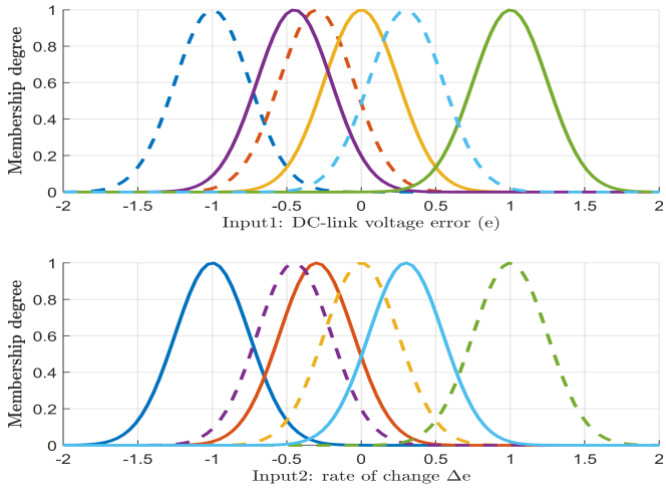

Fig. 3. Membership Functions for e and Δe Variables

3.2. Flower Pollination Optimization Method

Although it is true that each plant typically produces numerous flowers, and each floral patch has the potential to produce millions or even billions of pollen reproductive cells. To simplify, we suppose every single plant contains one blossom producing one pollen gamete, which we equate to a solution. The FPA is based on flowers and has two key steps: global and local pollination. Insects transport pollens during global pollination, which helps reproduce the fittest individuals (g∗). The first criteria and floral consistency are described as follow:

$$x_i^{t+1} = x_i^t + L(x_i^t - g_*) \tag{29}$$

In the context of a given iteration t, x_i^t represents either the pollen i or the solution vector x_i, while g∗ refers to the best solution found. To simulate the efficient movement of insects, we introduce the pollination strength parameter L. To effectively mimic this characteristic, a Levy flight distribution is used. Specifically, we use equation 30, which represents the probability density function of the symmetric Levy distribution with a characteristic exponent λ = 1.5, where s is a random variable.

$$L \sim \frac{\lambda\Gamma(\lambda)\sin\pi\lambda/2}{\pi}\frac{1}{|s|^{\lambda+1}} \tag{30}$$

The second rule may be stated as:

$$x_i^{t+1} = x_i^t + \epsilon\left(x_j^t - x_k^t\right) \tag{31}$$

x_j^t and x_k^t are designations given to pollens that come from distinct flowers of a particular plant species.

To provide an accurate depiction of the intricacies of pollination, the phenomenon of flower constancy, and the foraging patterns of pollinators, we can establish a set of definitive rules:

1) Pollen-carrying pollinators engaging in Lévy flights contribute to a global pollination process, encompassing both biotic and cross-pollination mechanisms.
2) Local pollination, on the other hand, is a result of abiotic and self-pollination and is considered as a local process.
3) Flower-constancy can be viewed as the likelihood of successful reproduction being directly related to the degree of similarity between two flowers.
4) The switch probability (p), which represents the degree of control over local and global pollination, ranges from 0 to 1.

The aforementioned pair of rules, in conjunction with the transition condition, could be consolidated into the following pseudo code, as depicted below.

Flower Pollination Algorithm (FPA)

Define the membership function to be optimized
Create n solutions with d dimensions
Generate a n-by-d matrix of values between 0 and 1
Identify optimal solution ***g**** *in the starting population*
Evaluate objective function for each solution
Set MaxGeneration), p (global pollination)
Initialize the iteration counter t to 1
while t *<= **MaxGeneration***
  Initialize the flower/pollen gamete index ***i*** *to* ***1***
  while i *<= **n** (Iterate over all the flowers/pollen)*
    if rand *< **p***
      L *= **levy (d, 1.5)** Draw a d-dim Lévy step*
      Calculate the new solution using global pollination $\boldsymbol{x_i^{t+1} = x_i^t + L(x_i^t - g_*)}$
    else
      Draw two distinct random indices ***j*** *and* ***k***
      Calculate the new solution using local pollination $\boldsymbol{x_i^{t+1} = x_i^t + \epsilon\left(x_j^t - x_k^t\right)}$
    end
    if obj *< **bestObj***
      Replace current with new solution.
    end
    Increment the flower/pollen gamete index ***i*** ***(i = i + 1)***
  end
  Get ***best objective*** *value and index in population*
  Set ***current best*** *as best in population*
  Increment the iteration counter ***t (t = t + 1)***

end

3.3. Optimization of T2FLC using flower pollination algorithm

The optimization of the T2FLC using the FPA is an important step towards improving the efficiency and reliability of wind power plants.
Objective function
The choice of objective function will depend on the specific problem being solved and the goals of the optimization. It is important to define the objective function carefully so that it captures all the important factors that need to be optimized. In the case of optimizing the T2FLC for voltage regulation of ASCG in wind power conversion plants, the objective function is designed to balance various factors such as:

1) Minimizing the DC-link voltage deviation from the desired set-point to guarantee the system's steady operation.
2) Maximizing performance tracking of the machine output voltage to ensure it follows the reference voltage accurately and quickly.
3) Minimizing the control effort to ensure efficient use of the system resources.
4) Minimizing the output voltage's total harmonic distortion (THD) to ensure high-quality power output.

The process of defining a suitable function is crucial for the implementation of the Flower Pollination Algorithm. In this study, a new performance criterion has been introduced and presented in (32).

$$\text{func} = \omega_1\varepsilon_1^2 + \omega_2(1-\varepsilon_2^2) + \omega_3\varepsilon_3^2 + \omega_4\varepsilon_4^2 \quad (32)$$

With:

$$\varepsilon_1 = \frac{V_{dc} - V_{dc}^*}{V_{dc}^{max}} \; ; \; \varepsilon_2 = \frac{V_{out} - V_{ref}}{V_{ref}^{max}} \; ; \; \varepsilon_3 = \frac{u}{u_{max}} \; ; \; \varepsilon_4 = \frac{THD}{THD_{max}} \quad (33)$$

Where:

V_{dc} : the actual DC-link voltage.
V_{dc}^* : the desired set-point for the DC-voltage.
V_{dc}^{max} : the maximum allowable DC-voltage.
V_{out} : the actual generator output voltage.
V_{ref} : the reference voltage for the generator output.
V_{ref}^{max} : the maximum allowable generator output voltage.
u : the control effort required to maintain the DC voltage.
u_{max} : the maximum allowable control effort.
THD : the output voltage's total harmonic distortion (THD)
THD_{max} : the maximum allowable THD.
$\omega_1, \omega_2, \omega_3, \omega_4$: the weighting coefficients that determine the relative importance of each objective function.

4. Comparative Matlab Simulation Analysis

This study introduces an inventive strategy for the regulation of the three-phase DC voltage rectifier, employing a type-2 fuzzy logic regulator based on Direct Power Control (DPC). To optimize the controller's performance, the antecedent and consequent parameters are determined using the flower pollination optimization method. Figure 4 showcases the recommended control structure. To assess its effectiveness, a comprehensive simulation model of the entire system is developed using MATLAB/Simulink.

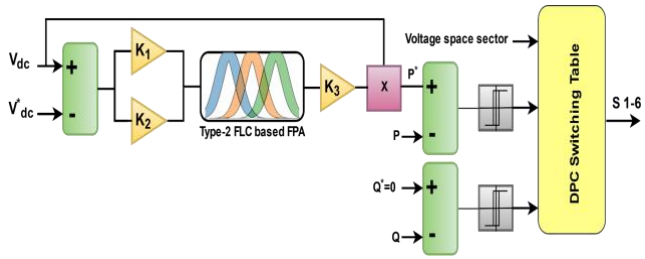

Fig. 4. The suggested framework for regulating a three-phase rectifier.

The Simulink model shown in Fig.5 consists of the ASCG machine that considers iron losses, an AC-DC converter, DC load, and a control block. Table 1 provides the parameters for this model.

Table 1. Simulation parameters for this study.

Parameters	Value
Angular velocity	314 rad/s
Excitation capacitors	70 µF
Inductance	1 mH
Resistance	0.1 Ω
DC- capacitance	4000 µF
DC loads	100 Ω

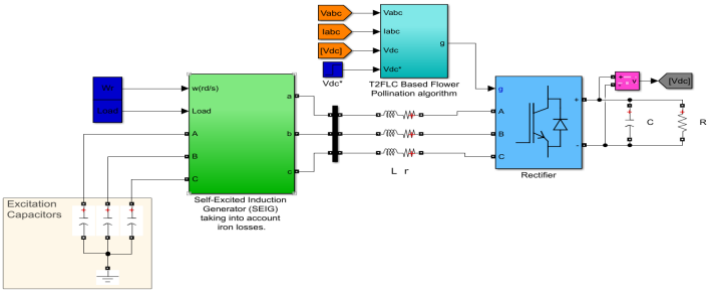

Fig.5. MATLAB/Simulink model of the entire system

An evaluation of the rectifier's performance is conducted using the suggested controller under three distinct operating circumstances. Numerous indicators are considered during the assessment: such as response time, stabilization time, excess amplitude, overall harmonic distortion, and power factor (PF). The designated operational requirements are enumerated underneath:

1. Condition 1: states that the input reference for this operating state remains fixed, with a reference command of 600 V being set before the rectifier begins functioning.
2. Condition 2: the rectifier's step response is analyzed while the DC voltage reaches a stable value. The DC voltage's reference is then altered from 600V to 800V, followed by a subsequent shift from 800 V back to 600 V.
3. Condition 3: wind change
4. Condition 4: investigates the effect of reducing the load by 50% (from 40Ω to 20Ω) on the rectifier's DC side.

4.1. Condition 1: Fixed VDC input reference

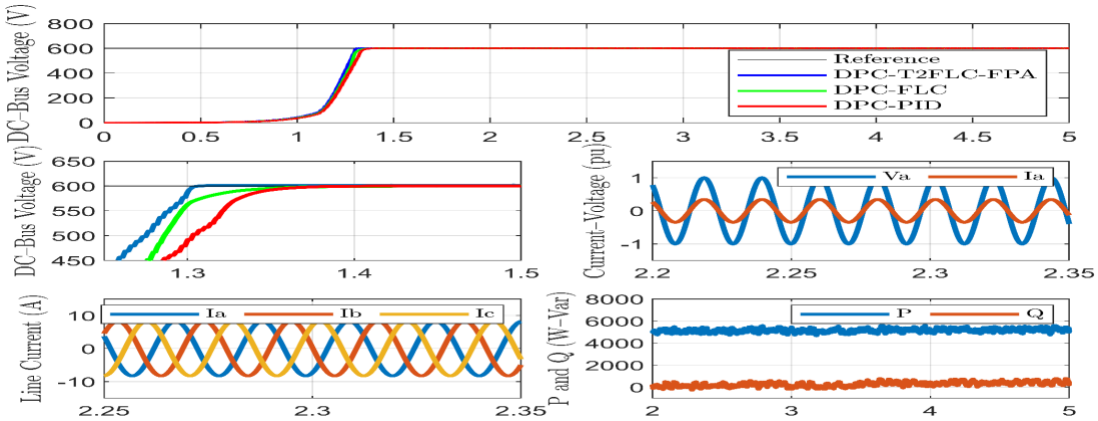

Fig. 6. The results from a simulation with a fixed target value.

Comparative results are provided for the DC-link voltage among three different controllers: DPC-T2FLC-FPA, DPC-FLC, and DPC-PI. However, only the DPC-T2FLC-FPA controller is evaluated for the other results. The response of the DC-link voltage, active and reactive powers, as well as the output voltage and current of the ASCG, to a constant input, is illustrated in Fig.6. Once the rectifier begins operating, all three controllers can achieve the DC-voltage reference value without any steady-state error or overshoot. Nevertheless, the DPC-T2FLC-FPA controller achieves the reference value for the DC-link voltage at a quicker pace. Furthermore, all three controllers ensure the continuity of a sinusoidal rectifier's input across transient and sustained modes, guaranteeing the smooth and uninterrupted flow of current.

Table 2. Controller Performance under Constant Reference.

Indicator of Performance	DPC-T2FLC-FPA	DPC-FLC	DPC-PID
T_r (s)	1.2349	1.2483	1.2581
T_s (s)	1.3071	1.3764	1.3813
M_p (%)	0	0	0
Cos phi	0.9998	0.9992	0.9989
THD (%)	2.77	2.92	3.19

Performance results for constant reference operation are presented in Table 2 for each controller. According to the table, the proposed controller improved the rise time, settling time, power factor (PF) and total harmonic distortion (THD) by 1.1%, 5.03%, 0.06%, and 5.14%, respectively, for the DPC-FLC controller. For the DPC-PID controller, the proposed controller also increased these parameters by 1.84%, 5.37%, 0.09%, and 13.16%, respectively. These enhancements are particularly valuable in scenarios with fixed V-DC input references, where rapid response times and improved power quality translate into more stable grid integration, reduced operational costs, and increased economic viability for renewable energy systems.

4.2. Condition 2: Varied input reference of VDC

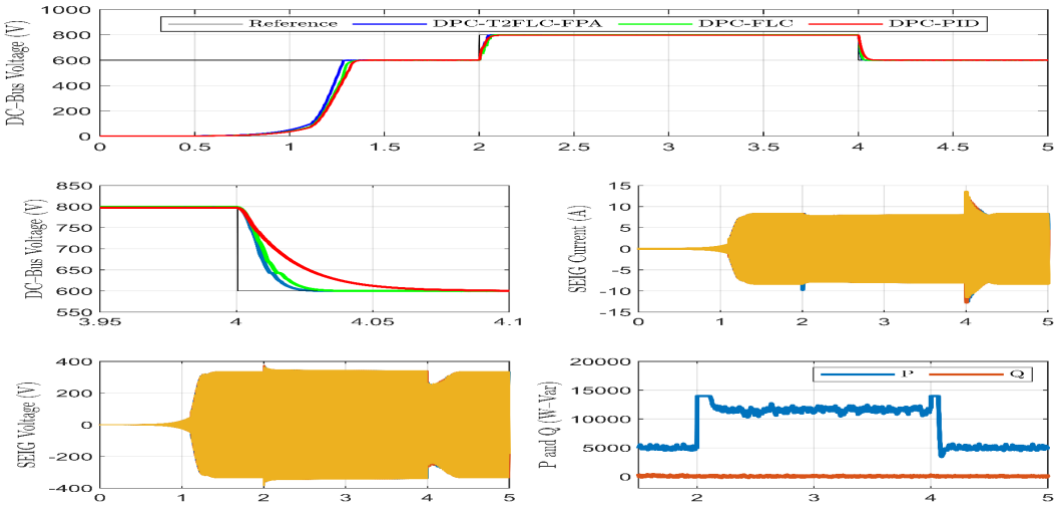

Fig. 7. Simulation outcomes of DC voltage variation.

The results of the system's response to a sudden voltage change are presented in Fig.7. The rectifier was in a stable state when the DC voltage's reference was raised from 600 Volt to 800 Volt at t = 2 s, then changed back to 600 V at t = 4 s. All three controllers successfully adjusted the voltage across the DC link to the chosen reference without making an equilibrium oversight or overshooting. The DPC-T2FLC-FPA controller exhibited a faster response in maintaining the reference value of the DC voltage than the other controllers. The results showed a linear relationship between the V-DC and the active power. Specifically, the DC-link voltage increased as more input power was drawn and decreased as less input power was drawn. Initially, the rectifier consumed 5000 W of active power within 2 seconds. At the 2-second mark, the reference V-DC was raised to 800 Volt, causing the rectifier to temporarily increase its active power usage to achieve the elevated V-DC. Once the V-DC reached its reference target, a new active power equilibrium was established for the ASCG. At t = 4 sec, the converter drew reverse active power to reduce the V-DC. This indicated that the DC-link capacitor was discharging, causing a proportional decrease in the V-DC. Furthermore, no reactive power variation during transient and steady states. Moreover, the three controllers maintain a sinusoidal shape of the converter input current and ensure a superior cos phi in both transitory and permeant modes. Table 3 outlines the performance requirements for every controller during a step change operation. In summary, our research results in the context of varying V-DC input references provide substantial practical insights, showcasing the controller's adaptability, reliability, and its direct applicability to a diverse range of industries and real-world scenarios.

Table 3. Controller Performance under Variable Reference.

Performance Criteria	DPC-T2FLC-FPA	DPC-FLC	DPC-PID
Ts (s) (600V to 800V)	1.2349	1.2483	1.2581
Ts (s) (800V to 600V)	1.3071	1.3764	1.3813
Mp (%)	0	0	0
PF(cos phi)	1	0.9997	0.9992

4.3. Condition 3: Varied wind speed

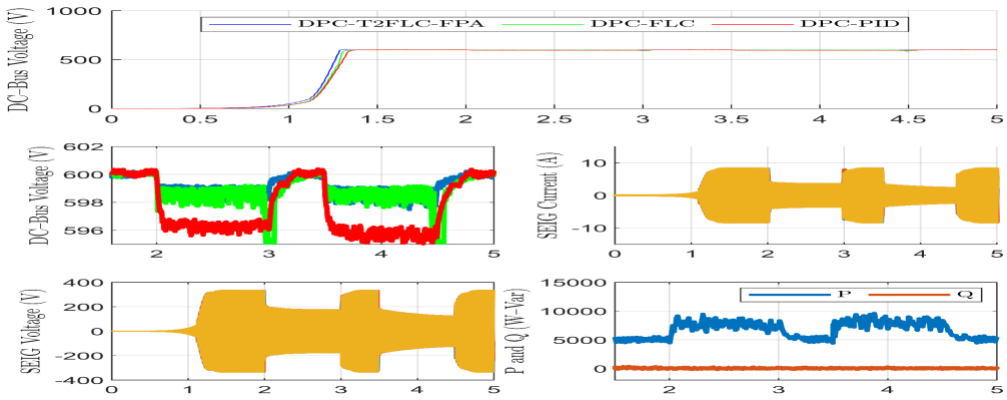

Fig. 8. Simulation outcomes of wind speed variation.

Figure 8 illustrates the outcomes of the system functioning in a scenario with fluctuating wind speeds. The wind speed undergoes changes between t = 2 s and t = 4.5 s while the rectifier is in a stable state. In all cases of the controller, the results indicate that the DC-link voltage fluctuates, and a minor static error is observed. Upon comparing the outcomes of all the controllers, it is evident that the error is minimized in the scenario where the DPC-FLC-FPA controller is utilized. The reactive power is found to be negligible, signifying a high-cos phi. After the fluctuation subsides, it's observed that the rectifier utilizing the DPC-FLC-FPA controller achieves a faster recuperation time for the V-DC. Table 4 displays the performance of each controller in the context of operation under varying wind speeds.

Table 4. Controller Performance under Variable Wind speed.

Performance Criteria	DPC-T2FLC-FPA	DPC-FLC	DPC-PID
T_{s1} (s)	3.1804	3.2145	3.4862
T_{s2} (s)	4.7059	4.7439	4.7605
M_p (%)	0	0	0
e_{ss} (V)	1	2	4
PF	1	0.9991	0.9988

The data presented in Table 4 indicates that all the controllers exhibit a notable power factor, indicating a high level of performance in this aspect. When contrasting the suggested controller with the remaining controllers (DPC-FLC and DPC-PID), the settling time (Ts1) enhancements for this specific condition are 1.1%, 9.61% respectively, and 0.8%, 11.6% respectively for (Ts2). In summary, our research on varied wind speeds offers practical benefits for renewable energy. Improved power factor and faster settling times enhance efficiency and cost-effectiveness in wind energy applications, benefiting industries like wind farms and remote installations. Our controller's adaptability and scalability make it a versatile solution for projects of all sizes, advancing sustainable wind energy systems.

4.4. Condition 4: Varied load on the DC side

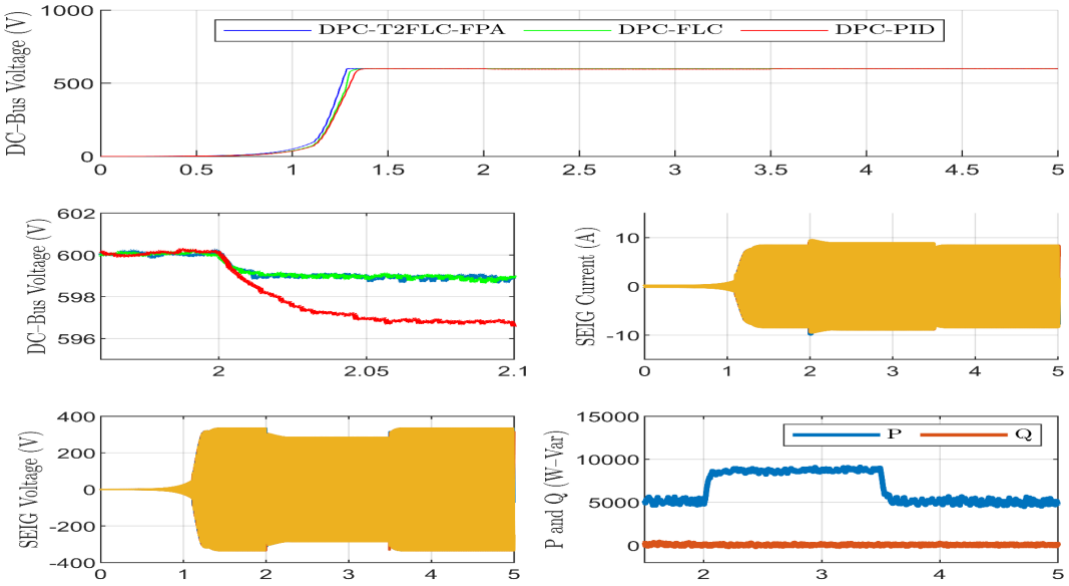

Figure. 9. Simulation outcomes of load variation.

Figure 9 displays the outcomes of the system when subjected to variations in load on the DC side. At t = 2 s, the DC-impedance load has undergone a decrease, shifting its resistance from 40 Ω to 20 Ω., and then at t = 3.5 s, it is raised back up from 20 Ω to 40 Ω. Each controller guarantees that the DC-V has no steady-state error. The converter's DC-voltage experiences both over and under-shoots when controlled by the DPC-T2FLC-FPA, DPC-FLC, and DPC-PID controllers. However, these over and under-shoots are comparatively smaller when using the DPC-T2FLC-FPA controller compared to the other two. Reducing the DC impedance load to 20 Ω at t = 2 s causes an increase in the current and active power drawn by the load, while maintaining a constant DC voltage. Between 2 s and 3.5 s, the rectifier draws a higher amount of active power from the self-excited induction generator, approximately 8500 W, compared to the 5000 W drawn up to 2 s. Furthermore, the DPC-T2FLC-FPA controller exhibits a shorter recovery time in comparison to the other controllers. In summary, our research on variable DC load conditions has practical implications. The controllers' improved power factor and reduced settling times offer energy efficiency gains and cost savings potential in applications with

dynamic loads, such as renewable energy and manufacturing. Rapid response to changing DC loads ensures stable power supply, crucial for operational efficiency and grid stability. The controller's adaptability and scalability make it versatile for various projects, enhancing power system reliability and efficiency in dynamic load scenarios.

5. CONCLUSION

The presented research introduces a novel and sophisticated control approach aimed at precise regulation of the DC-link voltage in three-phase Autonomous Squirrel Cage Generators (ASCGs). This cutting-edge approach combines the Direct Power Controller (DPC) with the advanced Type-2 Fuzzy Logic Controller (T2FLC), meticulously optimized through the implementation of the Flower Pollination Algorithm (FPA). Through extensive MATLAB simulations, the proposed controller surpasses the conventional Proportional-Integral (PI) and Type-1 Fuzzy Logic Controller (T1FLC) counterparts in various dynamic scenarios encompassing varying load and speed conditions. This superior performance observed in the ASCG's responses indicates a significant advancement in its overall operational efficiency.

The FPA optimization technique employed in this research plays a pivotal role in elevating the controller's performances (Tr, Ts, Mp, Cos phi, THD) to unprecedented levels, as it effectively enhances the regulation of the DC-link voltage. This optimization process, inspired by the fascinating mechanisms of flower pollination in nature, demonstrates its ability to extract optimal solutions by mimicking the natural phenomenon. The comprehensive findings of this study shed light on a highly promising and forward-thinking approach for DC-link voltage regulation in ASCGs integrated within renewable energy systems. These insights are expected to significantly benefit researchers and practitioners engaged in the dynamic and ever-evolving fields of power electronics and green energy plants, paving the way for further advancements in this domain.

References

[1] F. Ayadi, I. Colak, I. Garip, and H. Bulbul, ‘'Impacts of renewable energy resources in smart grid". 8th International Conference on Smart Grid (icSmartGrid), pp. 183-188. IEEE, June 2020.

[2] P. Pareek and H. D. Nguyen, “Probabilistic robust small-signal stability framework using gaussian process learning,” Electr. Power Syst. Res., vol.188, pp. 1–7, 2020.

[3] S. Leonelli and N. Tempini, "Data Journeys in the Sciences'‘. pp.412, Springer 2020.

[4] G. Nguyen, S. Dlugolinsky, M. Bobák, V. Tran,, Á. López García, I. Heredia and L. Hluchý,. "Machine learning and deep learning frameworks and libraries for large-scale data mining: a survey". Artificial Intelligence Review, 52, 77-124.2020.

[5] R. Vinayakumar, M. Alazab, K. P. Soman, P. Poornachandran, A. Al-Nemrat, and S. Venkatraman, “Deep Learning Approach for Intelligent Intrusion Detection System,” IEEE Access, vol. 7, pp. 41525–41550, 2019.

[6] K. Sivaraman, R. M. V. Krishnan, B. Sundarraj, and S. Sri Gowthem, “Network failure detection and diagnosis by analyzing syslog and SNS data: Applying big data analysis to network operations,” Int. J. Innov. Technol. Explor. Eng., vol. 8, no. 9 Special Issue 3, pp. 883–887, 2019.

[7] A. Michon Michal, M. Ibrahim Albayati, and M. Aliyu. "An Integrated Wind Turbine and Power Grid Mode." 11th International Conference on Smart Grid (icSmartGrid). IEEE, 2023.

[8] F. Al-Turjman, H. Zahmatkesh, and L. Mostarda, “Quantifying uncertainty in internet of medical things and big-data services using intelligence and deep learning,” IEEE Access, vol. 7, pp. 115749–115759, 2019.

[9] S. Kumar and M. Singh, “Big data analytics for healthcare industry: Impact, applications, and tools,” Big Data Min. Anal., vol. 2, no. 1, pp. 48–57, 2019.

[10] L. M. Ang, K. P. Seng, G. K. Ijemaru, and A. M. Zungeru, “Deployment of IoV for Smart Cities: Applications, Architecture, and Challenges,” IEEE Access, vol. 7, pp. 6473–6492, 2019.

[11] B. P. L. Lau, S. H. Marakkalage, Y. Zhou, , N. U. Hassan, C. Yuen, , M. Zhan, and U. X. Tan." A survey of data fusion in smart city applications". Information Fusion, vol-52, no 357 pp-374.2019.

[12] Y. Wu, Y,Chen, L.Wang, Y.Ye, Z. Liu, Y. Guo, & Y. Fu. "Large scale incremental learning". In Proceedings of the *IEEE/CVF* conference on computer vision and pattern recognition. pp. 374-382.2019

[13] H. Benbouhenni, Z. Boudjema, and A. Belaidi." Using three-level Fuzzy space vector modulation method to improve indirect vector control strategy of a DFIG based wind energy conversion systems". International Journal of Smart Grid, vol.2, no.3, pp. 155-171.2018.

[14] V. Palanisamy and R. Thirunavukarasu, “Implications of big data analytics in developing healthcare frameworks – A review,” J. King Saud Univ. - Comput. Inf. Sci., vol. 31, no. 4, pp. 415–425, 2019.

[15] J. Sadowski, “When data is capital: Datafication, accumulation, and extraction,” Big Data Soc., vol. 6, no. 1, pp. 1–12, 2019.

[16] J. R. Saura, B. R. Herraez, and A. Reyes-Menendez, “Comparing a traditional approach for financial brand communication analysis with a big data analytics technique,” IEEE Access, vol. 7, pp. 37100–37108, 2019.

[17] D. Nallaperuma, R. Nawaratne, T. Bandaragoda, A. Adikari, S. Nguyen, T. Kempitiya, and D.Pothuhera. "Online incremental machine learning platform for big data-driven smart traffic management". IEEE Transactions on Intelligent Transportation Systems, vol-20. no.12, pp. 4679-4690S.2019.

[18] S.Schulz, M. Becker, M. R. Groseclose, S. Schadt, and C. Hopf, “Advanced MALDI mass spectrometry

imaging in pharmaceutical research and drug development," Curr. Opin. Biotechnol., vol. 55, pp. 51–59, 2019.

[19] C. Shang and F. You, "Data Analytics and Machine Learning for Smart Process Manufacturing: Recent Advances and Perspectives in the Big Data Era," Engineering, vol. 5, no. 6, pp. 1010–1016, 2019.

[20] Y. Yu, M. Li, L. Liu, Y. Li, and J. Wang, "Clinical big data and deep learning: Applications, challenges, and future outlooks," Big Data Min. Anal., vol. 2, no. 4, pp. 288–305, 2019.

[21] M. Huang, W. Liu, T. Wang, H. Song, X. Li, and A. Liu, "A queuing delay utilization scheme for on-path service aggregation in services-oriented computing networks," IEEE Access, vol. 7, pp. 23816–23833, 2019.

[22] G. Xu, Y. Shi, X. Sun, and W. Shen, "Internet of things in marine environment monitoring: A review," Sensors (Switzerland), vol. 19, no. 7, pp. 1–21, 2019.

[23] M. Aqib, R. Mehmood, A. Alzahrani, I. Katib, A. Albeshri, and S. M. Altowaijri, "Smarter Traffic Prediction Using Big Data, In-Memory Computing, Deep Learning and GPUs," Sensors, vol. 19, no. 9, pp. 2206–2239, 2019.

[24] N. Stylos and J. Zwiegelaar, "Big Data as a Game Changer: How Does It Shape Business Intelligence Within a Tourism and Hospitality Industry Context?" in Big Data and Innovation in Tourism, Travel, and Hospitality, Singapore: Springer, pp. 163–181.2019.

[25] Q. Song, H. Ge, J. Caverlee, and X. Hu, "Tensor Completion Algorithms in Big Data Analytics," ACM Trans. Knowl. Discov. Data, vol. 13, no. 1, pp. 1–48, Jan. 2019.

[26] E. SMAEEL, A. Mohamed Adel. "Steady State Analysis of A wind Energy Driven Self Excited Induction Generator (SEIG)".8th International Conference on Smart Grid (icSmartGrid). IEEE, 2020. p. 101-108.2020.

[27] M. R.. Khan, M. F. Khan, and M. Sartaj : "Consideration of Dynamic Cross Saturation in Mathematical Modeling of an Asymmetrical Six-Phase SEIG for Wind Energy Applications". IEEE International Conference on Power Electronics, Smart Grid, and Renewable Energy (PESGRE).pp. 1-6. IEEE. January 2022.

[28] M.Basic, D. Vukadinovic, D. Lukac. "Analysis of an enhanced SEIG model including iron losses". In: WSEAS Proceedings of 6th International Conference EEESD. p. 37-43.2010 .

[29] T. N.Abbasian, and F. R. Salmasi. "A flux observer with online estimation of core loss and rotor resistances for induction motors." International Review of Electrical Engineering. pp-4.5.2009

[30] T. Ahmed, K. Nishida, and M. Nakaoka, "Advanced control of PWM converter with variable-speed induction generator". IEEE Transactions on Industry Applications, vol.42, No.4, pp. 934-945.2006.

[31] J. M. Mendel, and F. Liu. "Super-exponential convergence of the Karnik–Mendel algorithms for computing the centroid of an interval type-2 fuzzy set". IEEE Transactions on Fuzzy Systems, vol.15,no.2, pp 309-320.2007.

[32] L.A. Zadeh. "The concept of a linguistic variable and its application to approximate reasoning—I." Information sciences. vol.8, No.3 pp. 199-249.1975.

[33] C. Lazaroiu, R. Mariacristina, and D. Zaninelli. "Fuzzy logic to improve prosumer experience into a smart city." International Conference on Smart Grid (icSmartGrid). IEEE, 2018.